Journal of Colloid and Interface Science 440 (2015) 292–298

Contents lists available at ScienceDirect

Journal of Colloid and Interface Science

www.elsevier.com/locate/jcis

Computer simulations of charged colloids in confinement

Antonio M. Puertas [a,*], F. Javier de las Nieves [a], Alejandro Cuetos [b]

[a] Group of Complex Fluids Physics, Departamento de Física Aplicada, Universidad de Almería, 04120 Almería, Spain
[b] Departamento de Sistemas Físicos, Químicos y Naturales, Universidad Pablo de Olavide, 41013 Seville, Spain

ARTICLE INFO

Article history:
Received 1 July 2014
Accepted 25 October 2014
Available online 13 November 2014

Keywords:
Colloidal interactions
Montecarlo simulations
Primitive model
Umbrella sampling
DLVO theory
Confined colloids

ABSTRACT

We study by computer simulations the interaction between two similarly charged colloidal particles confined between parallel planes, in salt free conditions. Both the colloids and ions are simulated explicitly, in a fine-mesh lattice, and the electrostatic interaction is calculated using Ewald summation in two dimensions. The internal energy is measured by setting the colloidal particles at a given position and equilibrating the ions, whereas the free energy is obtained introducing a bias (attractive) potential between the colloids. Our results show that upon confining the system, the internal energy decreases, resulting in an attractive contribution to the interaction potential for large charges and strong confinement. However, the loss of entropy of the ions is the dominant mechanism in the interaction, irrespective of the confinement of the system. The interaction potential is therefore repulsive in all cases, and is well described by the DLVO functional form, but effective values have to be used for the interaction strength and Debye length.

1. Introduction

Experimental measurements by optical microscopy of the interaction between a pair of colloidal particles confined by two parallel plates were first performed around 20 years ago, and revealed a surprising attraction between like-charge particles in the low salt regime [1–5]. The range of the attraction was too long to be attributable to van der Waals forces, and defied the understanding of the interaction between charged colloids based on the mean field theory of Derjaguin and Landau and Verwey and Overbeek [6], DLVO. The experiments were questioned due to optical dispersions [7–9], but it has been argued that this corrections are not important enough to modify qualitatively the main results[10]. In bulk, however, these attractions were not found by similar experimental techniques [11–14], except close to walls of the cell [15,16] – some works, however, reported the presence of voids in bulk systems [17,18], identified as liquid–vapor coexistence, which must be provoked by an attractive interaction. Furthermore, it has been proved that the attractions in confined systems are thermodynamically self-consistent, as shown by the agreement of configurational and hyperconfigurational temperatures with the bulk temperature [14,19].

The unexpected observation of attractions between like-charged particles motivated intense development of theories and computer simulations. The DLVO theory which describes most of the phenomenology of charged colloids correctly, predicts a purely repulsive interaction between a pair of particles with the same charge. However, it has been theoretically rationalized that attractions can be caused by ionic correlations in bulk colloids (neglected within the DLVO theory), particularly in the strong coupling limit and extremely low salt concentrations[20–23]. The ion-colloid coupling is measured by the ratio $Z\lambda_B/\sigma$, where Z and σ are the colloid charge and diameter, respectively and λ_B is the Bjerrum length. The effective colloid-colloid attraction has an important entropic contribution, similar to the ionic condensation described by Manning [24,25], for large values of $Z\lambda_B/\sigma$. Computer simulations confirmed these findings reporting liquid–vapor coexistence in bulk systems, but due to computational limitations relatively small colloid with small charges were modeled (or ions with a large valency) [26–29], or solvents with low dielectric constant, resulting also in strong electrostatic coupling [30]. However, the more relevant case of large colloid and big charges, has not been tackled yet.

Specific theoretical models have been devised for the case of interacting particles close to walls. Sader and Chan showed that within the Poisson–Boltzmann (PB) theory, the interaction is repulsive in all circumstances [31,32], so that other effects must be introduced to explain the experimental results. Experimentally, it has been shown that attractive interactions are asymmetric with

* Corresponding author.
E-mail addresses: apuertas@ual.es (A.M. Puertas), fjnieves@ual.es (F.J. de las Nieves), acuemen@upo.es (A. Cuetos).

http://dx.doi.org/10.1016/j.jcis.2014.10.044
0021-9797/

respect to the sign of the colloidal charge, indicating specific ionic interactions, not accounted for in PB theory [33]. Lee and Ng [34] proposed a model where fluctuations within the ionic clouds result in high-order electric moments provoking a net attraction between particles (plus ionic clouds), similar to the net dipolar attraction observed in colloids in interfaces [35,36]. Their results, however, indicate that this attraction would appear only for very low charges, where fluctuations are more important [34]. The fluctuations in the number of ions in the ionic clouds, on the other hand, can induce an attractive contribution between the macroions, as shown by Chen and Lee [37]. Using a cell model, it was shown that the attraction arising from these fluctuations has a strength of the order of $1k_BT$, thus much smaller than all other contributions to the interaction energy [37]. Other effects of non-electrostatic origin have also been studied, such as hydrodynamic interactions close to walls [38] or the importance of dissolved gas [39]. Since many of these effects, including electrostatics in the strong-coupling limit, can induce attractive contributions to the total interaction potential, the problem is still an open question, as to which is the dominant contribution in every case, and the overall role played by electrostatics.

In a previous work, using simulations with biassed sampling, we showed that for a pair of unconfined colloidal particles with large charges, as high as $Z = 600e$, with e the elementary charge, and monovalent salt in water, the interaction is purely repulsive, due to the loss of entropy of the ions, which are electrostatically confined between the colloids at short separations [40]. This is in qualitative agreement with the DLVO theory, despite the neglect of ionic correlations ($Z\lambda_B/\sigma$ was varied from ~0.3 to ~5). That work, however, was focused in bulk colloids, while the attraction between like charged colloids has been reported mainly in confined situations. Thus, we extend our previous work to confined systems, with the same range of $Z\lambda_B/\sigma$, i.e. low and intermediate electrostatic coupling, to check if the attractions can arise from electrostatic interactions upon confining the system, in conditions where these attractions would not appear in bulk. In our simulations, the interactions are calculated with the Ewald summation technique in two dimensions. The internal electrostatic energy is calculated by fixing the colloids and equilibrating the ions, whereas the free energy is determined by introducing a bias attractive potential between them. Different colloidal charges, up to $Z = 500e$, are considered, without added salt in water at room conditions, and different confinements, down to $L_z = 1.1\sigma$, with σ the colloidal particle diameter. We find that the interaction is repulsive in all cases, dominated by the loss of ionic entropy when the colloids approach each other, as in the bulk case. The effect of the confinement is only quantitative, reducing the intensity of the repulsion (namely, the effective charge), but leaving its range unaffected.

2. Simulation details

Monte Carlo simulations in the canonical ensemble were run in a system consisting of two positively charged macroions of charge Ze, where e is the unit charge, and diameter σ, and $2Z$ counterions with charge $-e$, ensuring electroneutrality. Situations with additional added salt have not been considered in this work. The methods used here are very similar to the described in a previous work[40]; we refer there for more detailed explanations, and present here a review of the methodology. Technical aspects about the computer simulation of confined charged fluids will be discussed in detail.

The interaction between all the particles has been modeled using the primitive model. The particles interact through the Coulomb potential plus a repulsive core that prevents overlap between the particles when they are closer than a contact distance, $\sigma_{ij} = 0.5(\sigma_i + \sigma_j)$ with σ_i and σ_j the diameter of species i and j (colloid particle or ion). Hence, for two particles of species i and j the interaction is given by:

$$\beta U_{ij}(r_{ij}) = \begin{cases} \infty & r_{ij} \leqslant \sigma_{ij} \\ \frac{Z_i Z_j}{r_{ij}} \lambda_B & r_{ij} \geqslant \sigma_{ij}, \end{cases} \quad (1)$$

where $\sigma_{ij} = 0.5(\sigma_i + \sigma_j)$ is the contact distance between the centers, and $\beta = 1/k_BT$, with k_B and T the Boltzmann constant and temperature, respectively. The diameter of the ions is $\sigma/40$. The Bjerrum length is given by $\lambda_B = \beta e^2/\epsilon$.

Besides this, to model the confinement, two infinite, parallel, hard and non-conducting walls were located at coordinates $z = -0.5L_z$ and $z = 0.5L_z$ (we take the z-axis as perpendicular to the plates and L_α is the box-size in the x-axis). The interaction between a particle i and the walls is infinity if $z_i > 0.5L_z - \sigma_i/2$ or $z_i < -0.5L_z + \sigma_i/2$ and zero otherwise (z_i is the z-coordinate of particle i). Note that image charges are not considered, namely, the dielectric constant of the planes is equal to that of the medium between them. In doing so, we aim to isolate the effect of the confinement of the double layers on the interaction (although in the experimental case image charges might have a relevant contribution).

Simulations were done in a simulation box with dimensions $L_x \times L_y \times L_z$. Periodic boundary conditions are only applied in the x and y directions, but not in the z direction. This geometry has been described previously as *slab geometry* [41]. This situation is completely different from the bulk case[40], where the periodic boundary conditions are applied in the three directions and no confinement is considered. In all the simulations of this work we set $L_x = 25\sigma$ and $L_y = 10\sigma$, while L_z has been changed from $L_z = 7.5\sigma$, close to the bulk case, to $L_z = 1.1\sigma$, which is a stringent confinement. Some bulk cases ($L_z = 10\sigma$ and periodic boundary conditions in the three directions) are also reported, for the sake of comparison. The values of L_x and L_y have been taken large enough to model an isolated pair of particles, i.e. the periodic images have a small effect on the interaction between them. On the other hand, if the system is made much larger, the counter-ion concentration is so small that the double layers around the colloids hardly form.

In order to make a direct comparison with experimental values feasible, we discuss briefly the values of the relevant parameters in typical experimental units. For reference, we take a typical particle diameter of $\sigma = 100$ nm. The Bjerrum length is $\lambda_B = 0.7$ nm $= 0.007\sigma$, to mimic the conditions of water at room temperature, and the ion size is 2.5 nm (although the this differs from the typical size of monovalent ions, we expect that the essential characteristics of the effective colloid-colloid interaction are captured by our model, as further discussed below, keeping within the current computer limitations). The colloid concentration goes from $8 \cdot 10^{-4}\sigma^{-3} = 8 \cdot 10^{11}$ cm^{-3} in the bulk case to $7.27 \cdot 10^{-3}\sigma^{-3} = 7.27 \cdot 10^{12}$ cm^{-3} for $L_z = 1.1\sigma$. For $Z = 500$, the surface charge density is $159.16e\sigma^{-2} = 0.255$ μC/cm^2, and the counter-ion concentration ranges from $0.4\sigma^{-3} = 0.664$ μM in the bulk case to $3.63\sigma^{-3} = 6.04$ μM for $L_z = 1.1$. The colloid concentration is too large, compared to the experimental values, but to reduce it larger simulation boxes should be considered, which would also decrease the ionic concentration to unrealistic values.

As the interaction between the particles is mainly electrostatic, special techniques must be used to handle the long-range character of this interaction. An efficient solution for this problem is the Ewald summation method, that includes the contributions to the energy from particles in all the periodic images of the simulation box. The description of Ewald summation for a system with periodic boundary conditions in the three directions (EWD3D) can be found elsewhere [41,42]. However, when the system under

consideration is periodic in two directions, x and y, but not in the third one, z, (slab geometry) the standard three dimensional Ewald summation cannot be used, and some alternatives have been proposed [43,44]. One option is to replicate the simulation box periodically in the z-direction, and use the standard Ewald summation, with an additional correction due to a spurious dipolar contribution [41,45,43,46]. This method (EWD3DC) is easy to implement, and its computational efficiency is similar to the standard EWD3D method, but it has been reported that it could introduce artefacts in the results [44]. For this reason we have decided to implement the exact, but more expensive from a computational point of view, bi-dimensional Ewald summation (EWD2D). In this method, the expression of the electrostatic energy of the pair of particles i and j is given by [47–49]:

$$\begin{aligned}\frac{\beta U_{ij}}{\lambda_B} &= \frac{1}{2}\sum_{i,j=1}^{N}\sum_{|m|=0}^{\infty}{}' Z_i Z_j \frac{\operatorname{erfc}(\alpha|\mathbf{r}_{ij}+\mathbf{m}|)}{|\mathbf{r}_{ij}+\mathbf{m}|} \\ &+ \frac{\pi}{2A}\sum_{i,j=1}^{N}\sum_{\mathbf{h}\neq 0} Z_i Z_j \frac{\cos(\mathbf{r}_{ij}\cdot\mathbf{h})}{h}\left\{\exp(hz_{ij})\operatorname{erfc}\left(\alpha z_{ij}+\frac{h}{2\alpha}\right)\right. \\ &\left. + \exp(-hz_{ij})\operatorname{erfc}\left(-\alpha z_{ij}+\frac{h}{2\alpha}\right)\right\} \\ &- \frac{\pi}{A}\sum_{i,j=1}^{N} Z_i Z_j\left\{z_{ij}\operatorname{erf}(\alpha z_{ij}) + \frac{1}{\alpha\sqrt{\pi}}\exp(-\alpha^2 z_{ij}^2)\right\} - \left(\frac{\alpha}{\sqrt{\pi}}\right)\sum_{i=1}^{N} Z_i^2 \end{aligned} \quad (2)$$

where $\mathbf{m} = (m_x L_x, m_y L_y, 0)$ is the lattice vector with m_x and m_y integers. We also introduced the reciprocal lattice vector given by $\mathbf{h} = (2\pi m'_x/L_x, 2\pi m'_y/L_y, 0)$ with integers m'_x and m'_y, and the area of the unit cell $A = L_x L_y$. The primed sum in the first term indicates the omission of the $i = j$ term when $\mathbf{m} = 0$. α and the number of vectors $\mathbf{m}$ and $\mathbf{h}$ are adjustable parameters, chosen such that computational efficiency is optimized. $\operatorname{erf}(x)$ and $\operatorname{erfc}(x)$ denote the error function and the complementary error function, respectively. After several checks to ensure the convergence of the calculations we have used $\alpha L_z = 1$ and the number of vectors in Fourier space was fixed to 1256.

Due to the double sum over the particles in the Fourier part of the expression, the use of Eq. (2) has a very high computational cost. To overcome this problem, we have employed the technique proposed by Kumar and Panagiotopoulos [50] to speed up the calculations. There, the positions of the particles are constrained to a discrete cubic lattice, with small lattice spacing, a, and the interaction energy between all pairs of lattice sites is calculated only once at the beginning of the simulation. The lattice parameter is defined as $\chi = \sigma/a$ (the continuum limit is reached for $\chi \to \infty$). It has been shown previously that the results obtained with this method are independent on χ if this parameter is big enough [51]. Thus, we have used, as in our previous work [40], $\chi = 35$. Now the electrostatic interaction of Eq. (2) is pre-calculated only once at the beginning of the simulation and stored in an array. With this, it is possible to carry out simulations within reasonable computational time. Note that, because a lattice site can only be occupied by one ion (or colloid), the effective ionic size is given by the lattice parameter χ. Because the electrostatic energy is independent of χ above $\chi = 35$ [51], we expect that our results are independent of the ionic size, though it is certainly unrealistic.

With the general details described above, two different types of simulations have been carried out. In the first, the position of the two colloidal particles was fixed at coordinates $(-R/2, 0, 0)$ and $(R/2, 0, 0)$, whereas ions were allowed to change their positions in the lattice according to a standard Metropolis algorithm with a maximum displacement of 5σ. From random positions for all the ions, 10^5 Monte Carlo cycles were run to equilibrate the system – a cycle consists in $2Z$ trials to move a randomly chosen ion. From the thermalized configuration, 10^5 additional Monte Carlo cycles were run to obtain averages. Hence, with this method we calculated the internal energy of the system as a function of the distance between the colloidal particles, R, as well as the ionic density profile around them.

This method is useful to calculate the internal energy as a function of the distance between the colloids, but this cannot be considered equivalent to the effective interaction between the colloids. To calculate the effective potential, it is necessary to integrate all degrees of freedom of the ions in the Hamiltonian of the system. In the integration of these degrees of freedom, besides an energetic contribution, the entropic contribution must also be considered, i.e. the effective interaction between the colloids is equivalent to the increase (or decrease) of free energy of the fluid as a function of the distance between the colloidal particles.

The free energy of the system with the colloids at distance R, $F(R)$, via

$$F(R) - F_0 = -\frac{1}{k_B T}\, ln(P(R)) \quad (3)$$

where F_0 is an undetermined constant, and $P(R)$ is the probability to find the two colloids at distance R. In principle, it could be possible to calculate $P(R)$ in a Monte Carlo simulation where the colloids were free to move, allowing the system to explore all the phase space. However, when the colloids repel each other, the region of short distances is poorly explored statistically, requiring very long simulations to achieve enough statistics for the calculation of $F(R)$. To overcome this difficulty, we have proposed [40] a simulation method based in the use of umbrella sampling Monte Carlo simulations [52,41]. In this method, a bias external potential is introduced in order to favor configurations that are rarely visited, improving the statistics in the calculation of $P(R)$ for these configurations. At the end of the simulation the effect of this bias potential is removed from $P(R)$ [40]. In this way, we have run simulations where the two colloidal particles are free to perform Monte Carlo moves with the electrostatic interaction with all other charges and an external bias potential between the colloids given by:

$$\beta U_{bias} = K(R - R_0)^2 \quad (4)$$

with R the distance between the colloidal particles, K gives the strength of the bias potential and R_0 a distance of reference. A given selection of K and R_0 allows the particles to explore a window of distances, and to sample $P(R)$.

With these details, the simulation technique was implemented as follows. 10^4 Monte Carlo cycles have been run to equilibrate the system, and 10^4 cycles to obtain averages. Now a Monte Carlo cycle comprises a trial move for each colloid in any direction plus $2Z$ trials to move an ion chosen at random. As a Monte Carlo move of one colloid will have a high probability to be rejected due to overlaps with ions, we have used the swap move technique: ions that overlap with the new colloid position are moved into the space left empty by the displaced colloid [53,51]. The acceptance ratio of moves per colloid was maintained at 40% while the maximum displacement for microions was fixed at 5σ. The Monte Carlo moves described here are done with the inter–particle potential described previously for the calculation of the internal energy, Eq. (2). Besides this, the bias potential is applied at the end of each Monte Carlo cycle, accepting or rejecting the whole cycle according to the Metropolis rule. In this work, the value of K is in the range $1–50\sigma^{-2}$ while R_0 varies from 0 to 7σ.

At the end of the simulation, the effect of the bias potential must be removed, and $F(R)$ is calculated from the $P(R)$ obtained in each window. The free energy in different windows must then be connected, fitting the constant F_0 in each window, to result in a continuous function. One constant is still undetermined, which we fit to set the origin of the free energy at $R = 10\sigma$, i.e.

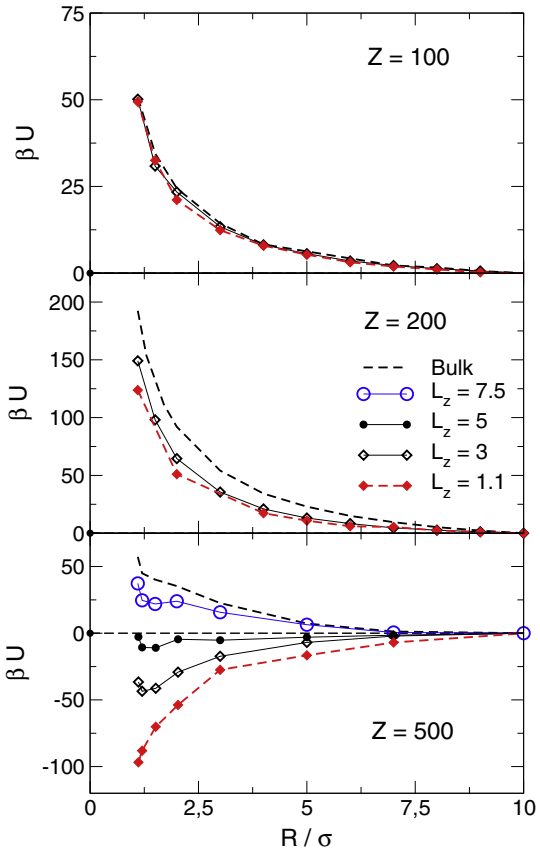

Fig. 1. Increase of the internal energy of the system with different colloid charges and separation between the confining planes, as labeled, from $R = 10\sigma$.

$F(10\sigma) = 0$. We refer to our previous work[40] for more details on this procedure.

3. Results and discussion

We start by presenting the internal electrostatic energy of the system, U, which is measured in simulations with the colloidal particles fixed; the confinement, in this case, affects only the ionic distribution around the colloids. Fig. 1 shows the internal energy as a function of the separation distance between the particles, increasing the confinement up to a separation between the planes of $L_z = 1.1\sigma$, with a constant number of counter-ions $n = 2Z$, i.e. without added salt (the internal energy is set to zero at $R = 10\sigma$). Three different colloid charges are considered: $Z = 100 < \sigma/\lambda_B$ (upper panel) where electrostatic coupling is weak, $Z = 200 \approx \sigma/\lambda_B$, (intermediate panel) where electrostatic and thermal energies are of the same order, and $Z = 500 > \sigma/\lambda_B$, (lower panel) where the electrostatics are expected to dominate. In bulk, the internal energy increases upon approaching the particles for the three charges studied, but when the confining planes approach each other, the energy decreases. This effect is weak at low colloidal charge, but it is clearly observed as Z grows. The case $Z = 500$ is particularly interesting: when the confinement is strong enough, the energy decreases as the colloids approach each other, implying an attractive contribution to the interaction potential induced solely by the modification of the ionic clouds. Note that this appears only when the electrostatic coupling is strong enough to form a condensed layer around the colloids.

A decrease of the internal energy upon approaching the colloid particles can also be observed in a bulk system when the colloid charge is increased well above the critical value $\sim \sigma/\lambda_B$ (upper panel of Fig. 2), although the total interaction potential between the colloids is always repulsive [40]. In the bulk case, the trend of the internal energy is originated by the competition between electrostatic coupling and ion entropy: upon increasing the charge, the ions are confined in the region between the colloids, decreasing the electrostatic energy. Similarly, when salt is added to the system (as shown in the lower panel of Fig. 2 for $Z = 500$), more ions are available to decrease the energy. The upturn of the energy at very small separation between the colloids, observed also in the confined systems (Fig. 1) is caused by the finite size of the ions, and has been described theoretically [22].

Thus, we study the ionic density distributions in bulk and in the confined systems. Fig. 3 shows the distributions for different separations between the colloidal particles and comparing the bulk and the confined systems for the strong coupling case, $Z = 500$ (the same scale is used in all plots; zenital and lateral views are presented for the confined system). The angular symmetry observed at large separations in the zenital view is lost when the colloids approach each other; the ions concentrate in the region between the two particles, thus reducing the electrostatic repulsion between the colloids. It is observed in the figure that the ionic concentration is larger when the system is confined, since the available space for the ions has reduced significantly, what explains the decrease of the internal energy in the confined case, as observed in Fig. 1. However, the electrical confinement is reduced to the region of maximum approach between the colloids, as shown in the lateral view, and is not affected by the planes. We also note in passing that ionic steric hindrance can be important in this region, particularly for large colloid charges, and must be considered in the models.

The ionic crowding can be quantified counting the ions around both colloids up to the coupling distance $Z\lambda_B$ (for $Z = 500$, $Z\lambda_B = 3.5\sigma$), N_B. For $L_z = 1.1\sigma, N_B \sim 290$ when the particles are far apart and $N_B \sim 580$ at closest distance, while in bulk the number of ions is $N_B \sim 190$ and $N_B \sim 440$ far apart and at closest distance,

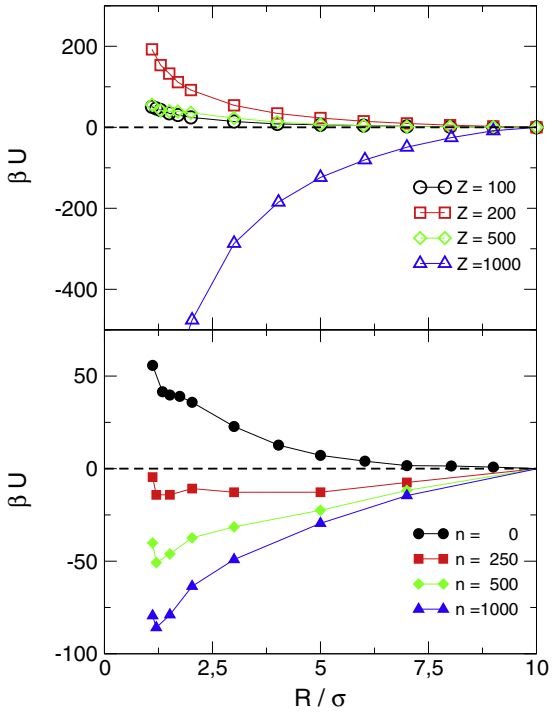

Fig. 2. Internal energy of the bulk system for different colloid charges (upper panel), and increasing the salt concentration with $Z = 500$ (lower panel).

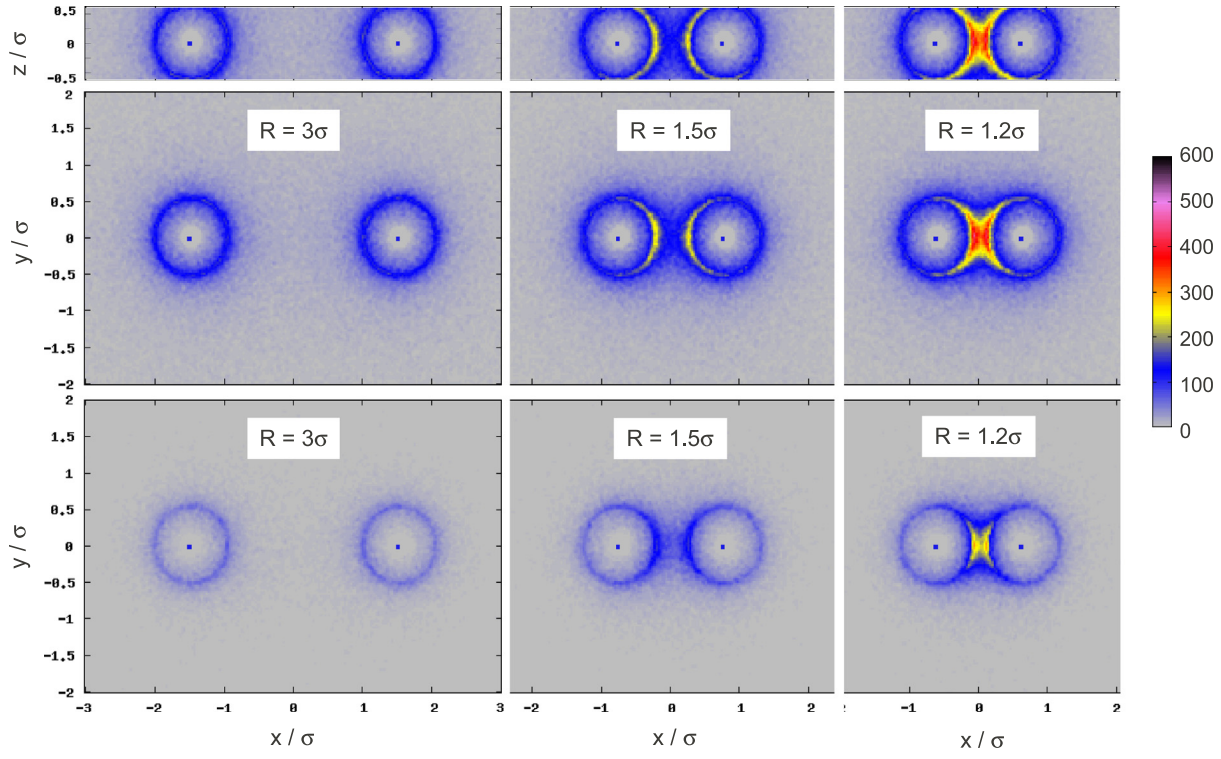

Fig. 3. Ionic density distributions for different colloid separations, as labeled, for a stringent confinement $L_z = 1.1\sigma$ (top rows; upper row is a lateral view and lower one a zenital view), and in bulk (bottom row), with $Z = 500$. The density is measured in units of ions per volume unit (σ^3), and the scale is the same for all plots, in the right.

respectively (at short separations, most of the counterions coupled to one colloid are also coupled to the other one, and thus are counted twice). Note that in all cases the total colloid charge ($2Z = 1000$) is not completely screened due to the balance between ionic coupling with diffusion. The fluctuations of the number of particles are relatively small, and thus not sufficient to provoke attractions of electric multipolar origin, as discussed by Lee and Ng [34]. We also note that our results concerning the ionic distributions are clearly different from the assumptions of Chen and Lee [37]; in their cell model, they assumed that the ionic clouds are isotropic and that the radial distribution functions are independent of the macroion separation, which is certainly not correct at small separations.

The effect of the ionic distribution on the interaction potential is accounted for by the ideal contribution to the entropy of the system. This is calculated as follows:

$$S_{id}/k_B = \int d^3\mathbf{r}\rho_c(\mathbf{r})(ln[4\pi\Lambda^3\rho_c(\mathbf{r})] - 1) \quad (5)$$

where $\rho_c(\mathbf{r})$ is the ion density, and Λ is the thermal de Broglie wavelength. The results for different charges and separations between the planes are shown in Fig. 4 (the entropy is set to zero at $R = 10\sigma$). Note that for large charges, where the colloid-ion electrostatic coupling is strong, the entropy decreases significantly upon approaching the colloids due to the dramatic increase of the ion concentration in the region between the colloids, resulting in a repulsive contribution for the free energy. This is not observed when the charge is lower, as the ions are almost free. (Note, however, that the internal energy yields a repulsive interaction in this case). Little influence is observed from the confinement, within the statistical uncertainty of the results, indicating again that the region where ions are electrostatically *trapped* between the colloids is not affected by the reduction of free space.

The total interaction potential between the colloids is given by the difference of free energy of the system, which we measure

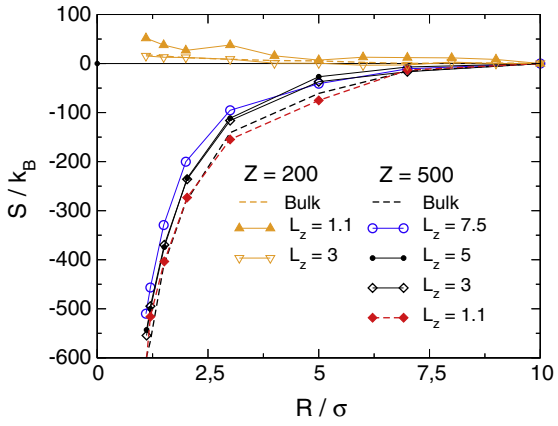

Fig. 4. Increase of the ideal contribution of the entropy for different colloid charges and confinements from $R = 10\sigma$, as labeled.

introducing an attractive bias potential, as explained above. The results are shown in Fig. 5 for different charges and separations between the planes. The interaction potential is repulsive in all cases, as expected from DLVO for colloids with similar charges, and more intense as the charge increases. It must be noted, nevertheless, that for low charges the dominant contribution is the internal energy, whereas for large charges the loss of entropy of the ions is much more important and drives the free energy. These results, therefore, indicate that the electrostatic interactions do not cause a net attraction between like-charge colloids with 1:1 salts in water.

The confinement reduces the strength of the repulsion, as noted in Fig. 5. However, this effect cannot be attributed to the increase of the ionic strength due to the reduction of accessible volume when the planes approach each other, as shown below. The

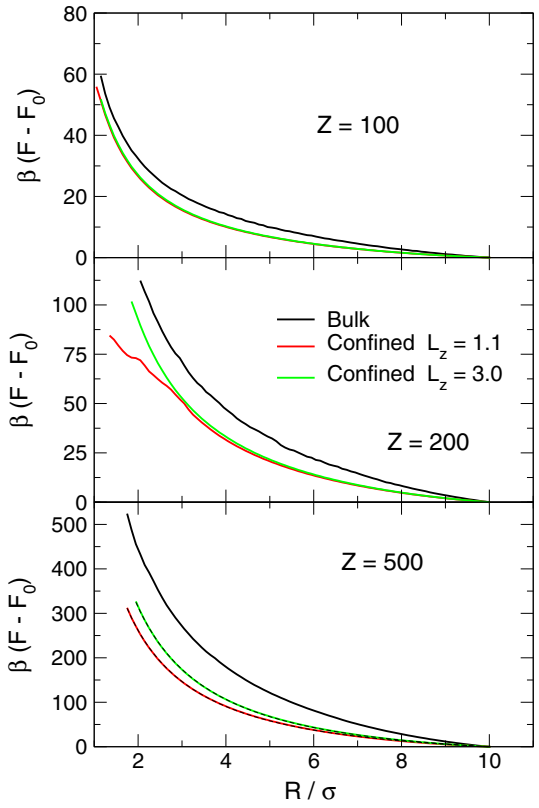

Fig. 5. Increase of the free energy of the system with different colloid charges and separation between the confining planes, as labeled. The dashed lines are the fittings of Yukawa potential, Eq. (6).

repulsive interaction between bulk colloids can be quite accurately described by the Yukawa functional form:

$$\beta u(r) = A_0 \frac{e^{-A_1 R}}{R} - A_0 \frac{e^{-10A_1}}{10} \tag{6}$$

where the second term has been added to yield $y(R = 10\sigma) = 0$, and allow comparison with our results. According to the DLVO theory,

$$A_0 = A_{DLVO} = Z^2 \left(\frac{exp[\kappa\sigma/2]}{1 + \kappa\sigma/2} \right)^2 \lambda_B, \tag{7}$$

is a measure of the effective charge of the colloids, and

$$A_1 = \kappa = \sqrt{\frac{e^2}{\epsilon k_B T} \sum \rho_i z_i^2}, \tag{8}$$

where ρ_i is the bulk ion density of species i (in our case, the summation contains only one term, corresponding to the counterions). Upon approaching the planes, the ionic strength increases and both A_0 and A_1 should increase. The Yukawa potential can be perfectly fitted to the results of both the bulk and confined systems, as shown in Fig. 5 for $Z = 500$ (dashed lines). It must be mentioned, however, that the DLVO theory does not account for the confining walls, so it is used here as an effective model, which describes correctly the results of the confined systems, and allows comparison with the bulk case. The parameters A_0 and A_1 used in the fittings are shown in Fig. 6 as a function of the theoretical κ, as calculated with the volume of the system, using Eq. (8). In the same figure, we present also the results for the bulk system with added salt ($n = 500$ and $n = 1000$ anion-cation pairs) [40].

For the bulk system, A_1 increases following the expected trend $A_1 = \kappa$ (marked by the dashed line), but A_0 decreases, contrary to the DLVO calculation. Upon confining the system, A_1 is almost

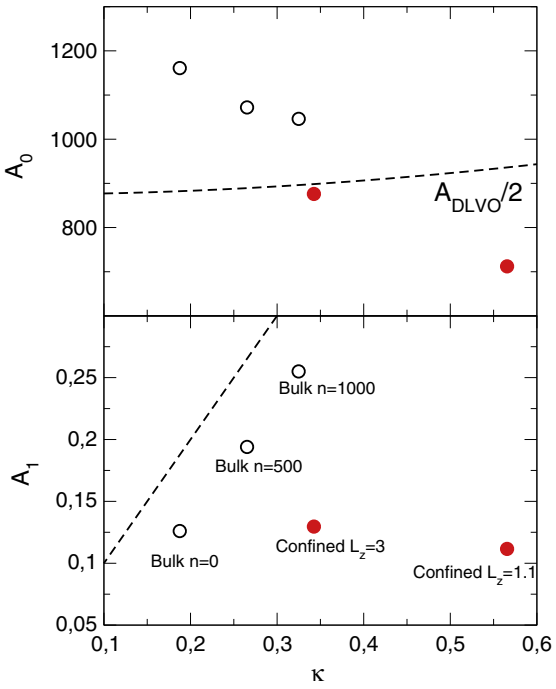

Fig. 6. Parameters of the Yukawa fitting to the interaction potential for $Z = 500$, A_0 and A_1, as a function of κ, calculated from Eq. (8). The line in the upper panel presents the theoretical trend (divided by 2) and the line in the lower panel corresponds to $A_1 = \kappa$.

unchanged from the bulk result, what cannot be explained simply by the increase of the ionic strength, and A_0 falls well below the expected result. These results imply that the range of the potential is similar for all cases, irrespective of the separation between the planes, and the effective charge decreases, what can be rationalized considering that the loss of configurational entropy of the ions, which is the dominant contribution for the free energy, is almost the same for all confinements, and the internal energy has the same decay length for all separations of the planes. To reduce the effective charge, ions must be tightly bounded to the colloid, what is favored by the confinement.

Finally, we would like to discuss some differences between our system and the experimental ones where attractions have been observed. The first difference concerns the particle charge; whereas we have focused here in a system with $Z = 500$, real colloids typically have larger charges, although our value is in the same order of magnitude. The effect that we observe here will be probably enhanced, but our present results do not allow us to conclude if attractions can appear at significantly larger charges. In any case, the trends observed in our study do not point in that direction.

Some experiments have reported attractions with modest salt concentrations, but not in fully deionized systems [7,8,10]. As in the case of bulk colloids, increasing the ionic concentration reduces the internal energy, making this attractive contribution more intense, but of shorter range. However, this is accounted for in the classical PB formalism, and thus we have concentrated in the region of low ionic concentrations, where PB is expected to fail more strongly. Another important aspect in connection with the experiments is the confining surfaces. Polin et al. [10] finds no attraction when the walls are conducting (and presumably uncharged). Wall charged with charges of the same sign of charge as the colloidal particles induce a stronger confinement, enhancing the effect found here. On the other hand, the combined modulation of the ionic density by charged walls and colloidal particles, can modify the effective interaction between the colloids observed here [10].

4. Conclusions

We have studied the problem of a pair of identical charged colloidal particles confined between two parallel plates by means of Monte Carlo simulations, as an approach to the experimental setup where attractions were reported. Besides a hard-core repulsion, only electrostatic interactions are considered in our simulations, calculated with the bi-dimensional Ewald summation technique. Colloid charges are varied from low values to the strong coupling regime, with monovalent counterions and without added salt, and the separation between the planes is varied down to $L_z = 1.1\sigma$. We have determined both the internal (electrostatic) energy, by fixing the colloids and equilibrating the ions, and the free energy, with the aid of a bias repulsive potential between the colloidal particles. The simulations have been performed in the canonical ensemble, but the experiments are performed in a system in contact with a salt solution, namely with constant ionic chemical potential. However, the fluctuations in the number of ions are very low, and the two ensembles yield similar results.

The interaction between the colloids, as given by the increase of the free energy from a reference distance, 10σ in our case, is repulsive for all confinements and colloid charges studied. At large charges, when the colloid-ion electrostatic coupling is important enough, the dominant contribution comes from the loss of ionic entropy, due to the electrostatic confinement of ions in the region between the colloids, what reduces the electrostatic energy. The confinement of the planes promotes this electrostatic effect, causing a reduction of the internal energy, but with minor effect on the loss of entropy. As a result, the effective interaction potential between the colloids is *less* repulsive upon confining the system, but is repulsive in all cases.

These results, therefore, linked with those obtained in our previous work [40] rule out electrostatic interactions as the possible origin of attractions between like charged colloids in water at room temperature, with counterions of low valency, in salt-free conditions and for the colloid charges here studied. However, it is shown here that the repulsion is less intense under confinement than in bulk. It is well known that multivalent ions with large colloid charges can indeed provoke effective attractions because of the strong ion-colloid coupling in bulk, and the confining planes can enhance this effect, and make it observable for ions of lower valency. Further work is needed closer to the experimental conditions, to attribute, or rule out, unambiguously if electrostatics can induce attractions between like-charged colloids. Still, other effects discussed in the literature, such as specific ionic interactions or hydrodynamics can be also responsible for attractions between like charged colloids.

Acknowledgments

The authors acknowledge financial support from Junta de Andalucía and FEDER under Project P09-FQM-4938 and Ministerio de Ciencia e Innovación (MICINN), through Project No. MAT2011-28385 (A.M.P.) and CTQ2012-32345 (A.C.).

References

[1] G.M. Kepler, S. Fraden, Phys. Rev. Lett. 73 (1994) 356.
[2] M.D. Carbajal-Tinoco, F. Castro-Román, J.L. Arauz-Lara, Phys. Rev. E 53 (1996) 3745.
[3] J.C. Crocker, D.G. Grier, Phys. Rev. Lett. 77 (1996) 1897.
[4] G.C. de León, J.M. Saucedo-Solorio, J.L. Arauz-Lara, Phys. Rev. Lett. 81 (1998) 1122.
[5] A. Ramírez-Saito, M. Chávez-Páez, J. Santana-Solano, J.L. Arauz-Lara, Phys. Rev. E 67 (2003) 050403.
[6] B. Derjaguin, L. Landau, Acta Physicochim. URSS 14 (1941) 633; J.W. Verwey, J.T.G. Overbeek, Theory of the Stability of Lyotropic Colloids, Elsevier, Amsterdam, 1948.
[7] J. Baumgartl, C. Bechinger, Europhys. Lett. 71 (2005) 487.
[8] J. Baumgartl, J.L. Arauz-Lara, C. Bechinger, Soft Matter 2 (2006) 631.
[9] M. Gygera, F. Rückerla, J.A. Käsa, J. Ruiz-García, J. Colloid Interface Sci. 326 (2008) 382.
[10] M. Polin, D.G. Grier, Y. Han, Phys. Rev. E 76 (2007) 041406.
[11] J.C. Crocker, D.G. Grier, Phys. Rev. Lett. 73 (1994) 352.
[12] J.C. Crocker, Nature 393 (1998) 621.
[13] M. Brunner, J. Dobnikar, H.H. von Grünberg, C. Bechinger, Phys. Rev. Lett. 92 (2004) 078301.
[14] Y. Han, D.G. Grier, J. Chem. Phys. 122 (2005) 064907.
[15] T. Muramoto, K. Ito, H. Kitano, J. Am. Chem. Soc. 119 (1997) 3592.
[16] M. Ishikawa, R. Kitano, Langmuir 26 (2010) 2438.
[17] K. Ito, H. Yoshida, N. Ise, Chem. Lett. 21 (1992) 2081; K. Ito, H. Yoshida, N. Ise, Science 263 (1994) 66.
[18] N. Ise, Phys. Chem. Chem. Phys. 12 (2010) 10279.
[19] Y. Han, D.G. Grier, Phys. Rev. Lett. 92 (2004) 148301.
[20] Y. Levin, Rep. Prog. Phys. 65 (2002) 1577.
[21] A. Naji, R.R. Netz, Eur. Phys. J. E 13 (2004) 43.
[22] A. Naji, S. Jungblut, A.G. Moreira, R.R. Netz, Physica A 352 (2005) 131.
[23] B. Zoetekouw, R. van Roij, Phys. Rev. Lett. 97 (2006) 258302.
[24] G.S. Manning, J. Chem. Phys. 51 (1969) 924.
[25] E. Trizac, L. Bocquet, M. Aubouy, Phys. Rev. Lett. 89 (2002) 248301.
[26] P. Linse, V. Lobaskin, J. Chem. Phys. 112 (2000) 3917.
[27] P. Linse, J. Chem. Phys. 113 (2000) 4359.
[28] J. Rescic, P. Linse, J. Chem. Phys. 114 (2001) 10131.
[29] A.V. Brukhno, T. Åkesson, B. Jösson, J. Phys. Chem. B 113 (2009) 6766.
[30] E. Allahyarov, E. Zaccarelli, F. Sciortino, P. Tartaglia, H. Löen, Europhys. Lett. 78 (2007) 38002. see also erratum 81, 59901 (2008).
[31] J.E. Sader, D.Y.C. Chan, J. Colloid Interface Sci. 213 (1999) 268.
[32] J.E. Sader, D.Y.C. Chan, Langmuir 16 (2000) 324.
[33] E.W. Gomez, N.G. Clack, H.-J. Wue, J.T. Groves, Soft Matter 5 (2009) 1931.
[34] C.-L. Lee, S.-K. Ng, J. Chem. Phys. 133 (2010) 084504.
[35] W. Chen, S. Tan, T.-K. Ng, W.T. Ford, P. Tong, Phys. Rev. Lett. 95 (2005) 218301.
[36] W. Chen, S. Tan, Z. Huang, T.-K. Ng, W.T. Ford, P. Tong, Phys. Rev. E 74 (2006) 021406.
[37] Y.-R. Chen, C.-L. Lee, Phys. Chem. Chem. Phys. 16 (2014) 297.
[38] T.M. Squires, M.P. Brenner, Phys. Rev. Lett. 85 (2000) 4976.
[39] M. Alfridsson, B. Ninham, S. Wall, Langmuir 16 (2000) 10087.
[40] A. Cuetos, J.A. Anta, A. Puertas, J. Chem. Phys. 133 (2010) 154906.
[41] D. Frenkel, B. Smit, Understanding Molecular Simulation: From Algorithms to Applications, second ed., Academic Press, 2002.
[42] M.P. Allen, D.J. Tildesley, Computer Simulation of Liquids, Clarendon Press, Oxford, 1987.
[43] P.S. Crozier, R.L. Rowley, E. Spohr, D. Henderson, J. Chem. Phys. 112 (2000) 3155.
[44] A. Cuetos, A.-P. Hynninen, J. Zwanikken, R. van Roij, M. Dijkstra, Phys. Rev. E 73 (2006) 061402.
[45] I.-C. Yeh, M.L. Berkowitz, J. Chem. Phys. 111 (1999) 3155.
[46] A. Grzybowski, E. Gwóźdź, A. Bródka, Phys. Rev. B 61 (2000) 6706.
[47] D.E. Parry, Surf. Sci. 55 (1976) 195.
[48] D.M. Heyes, M. Barber, J.H.R. Clarke, J. Chem. Soc. Faraday Trans. 2 (73) (1976) 1485.
[49] S.W. Leeuw, J.W. Perram, Mol. Phys. 37 (1979) 1313.
[50] A.Z. Panagiotopoulos, S.K. Kumar, Phys. Rev. Lett. 83 (1999) 2981.
[51] A.-P. Hynninen, M. Dijkstra, J. Chem. Phys. 123 (2005) 244902.
[52] G.M. Torrie, J.P. Valleau, J. Comp. Phys. 23 (1977) 187.
[53] V. Lobaskin, K. Qamhieh, J. Phys. Chem. B 107 (2003) 8022.